



Constraints on dark energy from TDCOSMO & SLACS lenses

Natalie B. Hogg  

Laboratoire Univers et Particules de Montpellier, Université de Montpellier, CNRS, Montpellier, France, 34090

Accepted 2024 January 8. Received 2023 December 3; in original form 2023 October 20.

ABSTRACT

Problems with the cosmological constant model of dark energy motivate the investigation of alternative scenarios. I make the first measurement of the dark energy equation of state using the hierarchical strong lensing time delay likelihood provided by TDCOSMO. I find that the combination of seven TDCOSMO lenses and 33 SLACS lenses is only able to provide a weak constraint on the dark energy equation of state, $w < -1.75$ at 68% confidence, which nevertheless implies the presence of a phantom dark energy component. When the strong lensing time delay data is combined with a collection of cosmic microwave background, baryon acoustic oscillation and Type Ia supernova data, I find that the equation of state is $w = -1.025 \pm 0.029$.

Key words: dark energy – gravitational lensing: strong

1 INTRODUCTION

The better part of three decades has passed since one of the most profound discoveries in modern cosmology was made: that the expansion rate of the Universe is currently accelerating (Riess et al. 1998; Perlmutter et al. 1999). In the standard model of cosmology, this acceleration is attributed to the cosmological constant Λ acting as a dark energy, with an equation of state $w = P/\rho = -1$, where P is the pressure and ρ the energy density of the dark energy. However, the true nature of dark energy, and in particular whether its energy density is actually constant in time, remains a subject of debate (Escamilla et al. 2023).

Various dark energy models have been proposed as alternatives to the cosmological constant, most of which incorporate a dark energy whose density changes over time (Copeland et al. 2006). A model-agnostic way of investigating this dynamical kind of dark energy is to use a parameterisation of the equation of state which allows for deviations from $w = -1$. A popular choice is the Chevallier–Polarski–Linder (CPL) parameterisation (Chevallier & Polarski 2001; Linder 2003),

$$w(a) = w_0 + (1 - a)w_a, \quad (1)$$

a first-order Taylor expansion in the scale factor a . The parameters w_0 and w_a can thus be constrained with data; deviations from $w_0 = -1$ and $w_a = 0$ would indicate that the energy density of dark energy is evolving in time.

Myriad observational data have been used to place constraints on the equation of state of dark energy. For example, the Planck satellite’s measurements of the cosmic microwave background (CMB) temperature anisotropies, E-mode polarisation and CMB lensing, along with baryon acoustic oscillations (BAO) measured by the 6dF Galaxy Survey and SDSS (Beutler et al. 2011; Ross et al. 2015; Alam et al. 2017) and the Pantheon catalogue of Type Ia supernovae (SNIa) (Scolnic et al. 2018), produced a measurement of $w = -1.028 \pm 0.031$ (Aghanim et al. 2020b). A stated goal of Stage IV

surveys such as Euclid is to measure the dark energy equation of state with percent-level precision (Amendola et al. 2018).

Strong lensing time delays are the measurement of the different arrival times of the multiple images of a gravitationally lensed source object (Refsdal 1964). This time delay depends on the angular diameter distances between the objects involved and thus directly probes the expansion rate of the Universe, H_0 . A distance ladder – a calibration of luminosity distances, typically to SNIa, using parallax measurements and the period–luminosity relation of Cepheid variable stars – is not needed to obtain cosmological information from strong lensing time delays, making them, on paper, a powerful probe of low-redshift cosmology.

Whilst there is no reliance on the distance ladder in strong lensing time delay measurements of H_0 , there can be a fairly significant dependence on how the mass profile of the lens galaxy is modelled (Sonnenfeld 2018). This problem has been recognised since the studies of the very first strongly lensed quasar for which time delays were measured, Q0957+561 (Walsh et al. 1979; Falco et al. 1985).

As an example of the effect of different lens modelling on the measurement of H_0 , we can compare the H0LiCOW measurement of $H_0 = 73.3^{+1.7}_{-1.8} \text{ km s}^{-1} \text{ Mpc}^{-1}$ (Wong et al. 2020), which comes from six strong lensing time delays and is a 2.4% precision measurement, with the TDCOSMO measurement, $H_0 = 74.5^{+5.6}_{-6.1} \text{ km s}^{-1} \text{ Mpc}^{-1}$ (Birrer et al. 2020), which comes from the original six H0LiCOW lenses plus one new lens and is a 9% precision measurement.

The reduction in precision is mainly the result of relaxing certain assumptions in the H0LiCOW lens modelling, namely making a choice of parameterisation for the lens mass profiles which is maximally degenerate with the so-called mass–sheet degeneracy, which I explain further below. To combat this increase in uncertainty, the TDCOSMO team added 33 additional lenses from the SLACS catalogue in order to provide more information on the mass profiles of the TDCOSMO lenses. This data and its nuisance parameters were combined with the original seven lens dataset in a hierarchical Bayesian manner, leading to a measurement of $H_0 = 67.4^{+4.1}_{-3.2} \text{ km s}^{-1} \text{ Mpc}^{-1}$,

* E-mail: natalie.hogg@lupm.in2p3.fr

which is in statistical agreement with both the H0LiCOW measurement and the measurement from the seven TDCOSMO lenses alone.

While [Lewis & Ibata \(2002\)](#) studied the theoretical effect of dynamical dark energy on strong lensing time delay measurements of H_0 , and the TDCOSMO H_0 value itself has been used to constrain variations of the fine structure constant ([Colaço et al. 2021](#)), axion–photon couplings ([Buen-Abad et al. 2022](#)) and interacting dark energy models ([Wang et al. 2022](#)), the full likelihood of [Birrner et al. \(2020\)](#) has not yet been used to obtain cosmological constraints beyond those on H_0 and the matter density parameter Ω_m . The H0LiCOW likelihood of [Wong et al. \(2020\)](#) was used to obtain constraints on various extensions to Λ CDM, including dynamical dark energy, with the previously alluded to caveat that the mass–sheet degeneracy was only broken by the assumption of certain analytic mass density profiles for the time delay lenses, a potential pitfall which the TDCOSMO likelihood avoids.

In this work, I present the first constraint on the dark energy equation of state using the full hierarchical TDCOSMO likelihood. Strong lensing time delays are particularly useful for this task as the constraints in the $w - \Omega_m$ plane are typically orthogonal to those coming from standard rulers i.e. the CMB and BAO ([Motta et al. 2021](#)). I begin by reviewing strong lensing time delays and the construction of the hierarchical TDCOSMO likelihood. I explain my analysis method and then present my results and conclusions.

2 STRONG LENSING TIME DELAYS

2.1 Theory

Gravitational lensing is the phenomenon which arises due to the deflection of light by massive objects. The strong lensing regime may be defined as that in which multiple images of a single source are produced. This typically occurs on super-galactic scales, with lenses being galaxies and sources being distant and bright objects such as quasars.

Light from the distant source is deflected by the lens galaxy. Different light paths have different lengths, leading to measurable delays between the arrival times of images. This strong lensing time delay is given by

$$t(\boldsymbol{\theta}, \boldsymbol{\beta}) = \frac{(1 + z_{\text{od}})}{c} \frac{D_{\text{od}} D_{\text{os}}}{D_{\text{ds}}} \left[\frac{(\boldsymbol{\theta} - \boldsymbol{\beta})^2}{2} - \psi(\boldsymbol{\theta}) \right], \quad (2)$$

where z_{od} is the redshift of the deflector; D_{od} , D_{os} and D_{ds} are the angular diameter distances between the observer and deflector, observer and source and deflector and source; $\boldsymbol{\theta}$ is the observed image position; $\boldsymbol{\beta}$ is the unknown source position; and $\psi(\boldsymbol{\theta})$ is the lensing potential, which carries the information about the mass density profile of the deflector. In a spatially flat Universe ($\Omega_k = 0$), the time delay is inversely proportional to H_0 via the angular diameter distances involved,

$$D(z) = \frac{c}{H_0(1+z)} \int_0^z \frac{dz'}{E(z')}, \quad (3)$$

where $E(z) \equiv H(z)/H_0$ is the dimensionless Hubble rate.

The difficulty faced by all strong lensing time delay inference is that under any arbitrary linear re-scaling of the source position $\boldsymbol{\beta} \rightarrow \lambda\boldsymbol{\beta}$, image positions $\boldsymbol{\theta}$ are preserved. The lens model is also accordingly transformed, $\boldsymbol{\alpha} \rightarrow \lambda\boldsymbol{\alpha} + (1-\lambda)\boldsymbol{\theta}$, where $\boldsymbol{\alpha}$ is the deflection angle. This is known as the internal mass–sheet transform or degeneracy ([Falco et al. 1985](#); [Schneider & Sluse 2013, 2014](#)). The only way that such a degeneracy can be broken and a measurement of H_0 made is by obtaining direct knowledge either of the absolute source size or of the

lensing potential itself. The former may be possible by measuring the size of quasar accretion disks using microlensing, but this technique comes with its own difficulties ([Chan et al. 2021](#)), so in order to reliably constrain H_0 a choice must be made in how to model the deflector mass density profile.

2.2 The TDCOSMO likelihood

Whilst the H0LiCOW team used analytic mass profiles for the deflectors to break the mass-sheet degeneracy, the TDCOSMO work used stellar kinematics data to provide information about the lensing potential. This led to the initial reduction in precision of the H_0 measurement compared to the H0LiCOW result. The precision was increased again by the addition of further stellar kinematics data from a set of 33 SLACS lenses, specifically selected for their similarity to the original seven TDCOSMO lenses. Note that these additional lenses do not have time delay information. Furthermore, the combination of data was made under the assumption that the TDCOSMO and SLACS lenses were drawn from the same parent population.

The complete likelihood describing this dataset was constructed hierarchically, meaning that a set of hyperparameters were defined which allowed all constraints related to the mass-sheet degeneracy to be inferred on a population level, whilst the lens and light model parameters, ξ_{mass} and ξ_{light} , could be inferred on a lens-by-lens basis. Thus, all remaining uncertainty about the mass-sheet degeneracy is propagated to the level of the H_0 inference.

Following [Birrner et al. \(2020\)](#), the posterior distribution of the cosmological parameters of interest, $\boldsymbol{\pi}$, given N sets of individual lens data \mathcal{D}_i and the model parameters $\boldsymbol{\xi}$, is given by

$$\begin{aligned} P(\boldsymbol{\pi}|\{\mathcal{D}_i\}_N) &\propto \mathcal{L}(\{\mathcal{D}_i\}_N|\boldsymbol{\pi})P(\boldsymbol{\pi}) \\ &= \int \mathcal{L}(\{\mathcal{D}_i\}_N|\boldsymbol{\pi}, \boldsymbol{\xi})P(\boldsymbol{\pi}, \boldsymbol{\xi}), \\ &= \int \prod_i^N \mathcal{L}(\mathcal{D}_i|\boldsymbol{\pi}, \boldsymbol{\xi})P(\boldsymbol{\pi}, \boldsymbol{\xi}). \end{aligned} \quad (4)$$

The nuisance parameter $\boldsymbol{\xi}$ is divided into the mass and light model parameters which are constrained at the level of each individual lens, and the set of mass-sheet degeneracy hyperparameters which are constrained at the population level, ξ_{pop} . The hierarchical TDCOSMO likelihood is thus given by

$$\begin{aligned} \mathcal{L}(\mathcal{D}_i|D, \xi_{\text{pop}}) &= \int \mathcal{L}(\mathcal{D}_i|D, \xi_{\text{pop}}, \xi_{\text{mass}}, \xi_{\text{light}}) \\ &\quad \times P(\xi_{\text{mass}}, \xi_{\text{light}}) d\xi_{\text{mass}} d\xi_{\text{light}}, \end{aligned} \quad (5)$$

where D is the set of angular diameter distances $\{D_{\text{od}}, D_{\text{os}}, D_{\text{ds}}\}$ from which all cosmological results are obtained. For a complete discussion of the construction of the hierarchical likelihood, including the details of the population hyperparameters, I refer the reader to Section 3 of [Birrner et al. \(2020\)](#).

The TDCOSMO measurement of $H_0 = 67.4^{+4.1}_{-3.2} \text{ km s}^{-1} \text{ Mpc}^{-1}$ is thus the most precise measurement possible from strong lensing time delays which does not make any assumptions about the deflector mass profiles in order to artificially break the mass-sheet degeneracy. It is also the first strong lensing time delay measurement of H_0 which used information from other datasets to improve the precision of the measurement. I will now discuss how I used this hierarchical likelihood to measure the dark energy equation of state.

3 METHOD

I wrote an external likelihood package for the cosmological modelling and sampling software Cobaya (Torrado & Lewis 2021), so that the hierarchical TDCOSMO likelihood can be used to obtain constraints on cosmological model parameters in combination with any other cosmological likelihood and with any choice of Boltzmann code. This package is publicly available.¹

Using the Markov chain Monte Carlo sampler provided by Cobaya, which is adapted from CosmoMC (Lewis & Bridle 2002; Lewis 2013) and uses a fast-dragging procedure to increase sampling speed (Neal 2005), I obtained constraints on three cosmological models: Λ CDM, w CDM and w_0w_a CDM. The w CDM model allows for a dark energy with a constant equation of state that may differ from $w = -1$; the w_0w_a CDM model allows for a dynamical dark energy. In a w CDM cosmology (extendable to w_0w_a CDM by the CPL parameterisation shown in Equation 1), and recalling that I keep $\Omega_k = 0$, the dimensionless Hubble rate is given by

$$E(z) = \left[\Omega_m(1+z)^3 + \Omega_{\text{DE}}(1+z)^{3(1+w)} \right]^{\frac{1}{2}}, \quad (6)$$

where $\Omega_m = \Omega_b + \Omega_c$, the sum of the baryon and cold dark matter densities, and Ω_{DE} is the dimensionless energy density of dark energy today.

For each cosmological model I considered, I sampled the posterior distributions of H_0 , $\Omega_b h^2$ and $\Omega_c h^2$, along with the relevant dark energy equation of state parameter(s). In each case, I also sampled the posterior distributions of the hyperparameters associated with the likelihood, and marginalised over them to obtain the posterior distributions on the cosmological parameters of interest. The computation of the angular diameter distances required by the TDCOSMO likelihood was done using the Boltzmann code CAMB (Lewis et al. 2000; Howlett et al. 2012), but I emphasise that I designed the Cobaya interface so that any theory code currently available in or added to Cobaya in the future can be used for this task. Lastly, I used the Parameterised Post-Friedmann framework in CAMB to allow w to cross -1 (Fang et al. 2008).

I validated my implementation of the likelihood package in Cobaya by comparing my Λ CDM results with the original TDCOSMO results, finding an excellent agreement in terms of constraints on both the cosmological and the nuisance parameters. This validation test, plus all of the code needed to reproduce the results and figures in this paper is also publicly available.²

Besides the TDCOSMO and SLACS datasets, I also obtained constraints on the models with a dataset consisting of the Planck 2018 measurements of the CMB temperature, polarisation and lensing (Aghanim et al. 2020a,c); the BAO measurements from the 6dF Galaxy Survey (Beutler et al. 2011), the SDSS Main Galaxy Sample (Ross et al. 2015) and the SDSS DR12 consensus catalogue (Alam et al. 2017); the Pantheon catalogue of Type Ia supernovae (Scolnic et al. 2018); and the TDCOSMO + SLACS lenses, in order to compare with the constraints obtained just using the strong lensing time delay data and with those of the Planck collaboration (Aghanim et al. 2020b). I will refer to this combination of data as the ‘‘full combination’’ from now on.

The priors I used for the cosmological parameters are listed in Table 1. Following Birrer et al. (2020), I also used the Pantheon prior on $\Omega_m = \mathcal{N}(0.298, 0.022)$ when using the TDCOSMO and SLACS data alone, though it is important to note that in my analysis Ω_m

| Parameter | Prior |
|--|------------------------|
| $\Omega_b h^2$ | [0.005, 0.1] |
| $\Omega_c h^2$ | [0.001, 0.99] |
| H_0 [kms ⁻¹ Mpc ⁻¹] | [0, 150] |
| w and w_0 | $[-3.0, -\frac{1}{3}]$ |
| w_a | [-4.0, 4.0] |

Table 1. Prior ranges of the parameters sampled in my analysis.

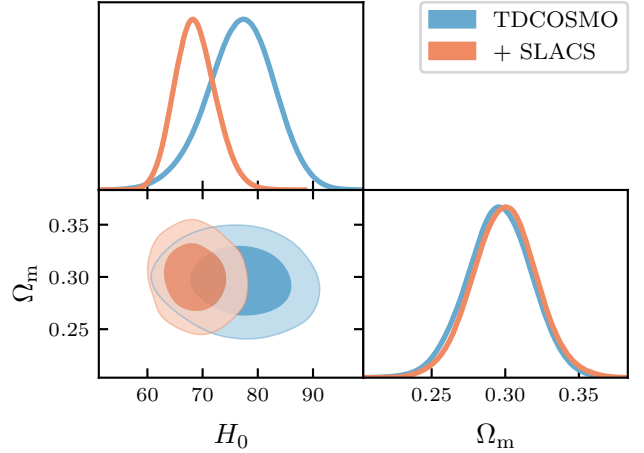


Figure 1. The one and two-dimensional marginalised posterior distributions of H_0 [kms⁻¹Mpc⁻¹] and Ω_m in a Λ CDM cosmology from the seven TDCOSMO lenses (blue) and the seven TDCOSMO + 33 SLACS lenses (red).

was not directly sampled since it is treated as a derived parameter in CAMB, the posterior being obtained from those of Ω_b and Ω_c . In the dynamical dark energy cases, I ensured that acceleration occurs by setting a prior on the dark energy equation of state such that $w < -\frac{1}{3}$.

4 RESULTS

In this section, I present the constraints obtained on Λ CDM, w CDM and w_0w_a CDM using the hierarchical TDCOSMO likelihood and the full combination of data listed above. Given the smaller uncertainty on H_0 that comes from combining the TDCOSMO + SLACS lenses, I will only present the TDCOSMO alone results for Λ CDM, to demonstrate the replication of Birrer et al. (2020). For the rest of the results, I will show constraints obtained using the complete TDCOSMO + SLACS dataset of 40 lenses. I used GetDist to make the figures and to compute the marginalised parameter values quoted in the text (Lewis 2019). The dark shaded regions of the contour plots represent the 68% confidence limit and the light shaded regions the 95% confidence limit.

4.1 Λ CDM

In Figure 1, I show the one and two-dimensional marginalised posterior distributions of H_0 and Ω_m in a Λ CDM cosmology. The blue contours show the constraints from the seven TDCOSMO lenses

¹ https://github.com/nataliehoggt/tocosmo_ext.

² <https://github.com/nataliehoggt/slide>.

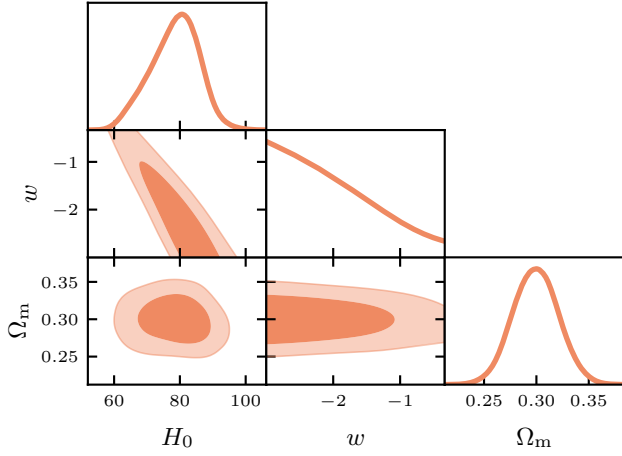


Figure 2. The one and two-dimensional marginalised posterior distributions of H_0 [$\text{kms}^{-1}\text{Mpc}^{-1}$], w and Ω_m in a w CDM cosmology from the seven TDCOSMO + 33 SLACS lenses.

alone, whilst the red contours show the constraints from the full dataset of 40 lenses (seven TDCOSMO + 33 SLACS lenses). As expected, this result replicates the findings of the TDCOSMO paper, with $H_0 = 76.8^{+6.4}_{-5.6} \text{kms}^{-1}\text{Mpc}^{-1}$ from the TDCOSMO lenses and $H_0 = 68.7^{+3.4}_{-3.9}$ from the TDCOSMO + SLACS lenses. These values are fully consistent at 1σ with the TDCOSMO result.

4.2 w CDM

In Figure 2, I show the one and two-dimensional marginalised posterior distributions of H_0 , w and Ω_m in a w CDM cosmology from the seven TDCOSMO + 33 SLACS lenses. The likelihood is able to provide a weak constraint on the equation of state of dark energy, $w < -1.75$ at 68% confidence, which implies that the dark energy is ‘phantom’, the term applied when $w < -1$.

Some consideration must be given here to what is, at first glance, a surprising result. It is known that in some datasets, such as Planck 2018, large negative values of w correlate with large positive values of H_0 (Escamilla et al. 2023). This is due to the so-called geometrical degeneracy, where H_0 , Ω_m and w can take various values which in combination lead to the same value for the angular diameter distance to the surface of last scattering and hence the same angular size of the sound horizon, provided the physical sound horizon size is kept fixed (Efstathiou & Bond 1999).

Since strong lensing time delays also rely on angular diameter distances to probe cosmology, I infer that a similar degeneracy exists here. This conclusion is supported by the clear correlation between H_0 and w in Figure 2. Thus, the strongly negative dark energy equation of state is likely driven by the high central value of $H_0 = 78.4^{+8.3}_{-6.3}$ obtained in this case – which is nevertheless consistent with the Λ CDM value at 1σ . Furthermore, the 95% confidence limit is $w < -0.74$, reflecting the broadness of the constraint obtained. As expected, based on the results of Birrer et al. (2020), the marginalised posterior value of the matter density $\Omega_m = 0.299 \pm 0.022$ is largely informed by the Pantheon prior. This also acts to somewhat ameliorate the aforementioned degeneracy.

Lastly, I note that a deeply phantom equation of state (for this value of Ω_m , $w \lesssim -1.4$) corresponds to a violation of the null energy condition (Colgáin & Sheikh-Jabbari 2021), which may be

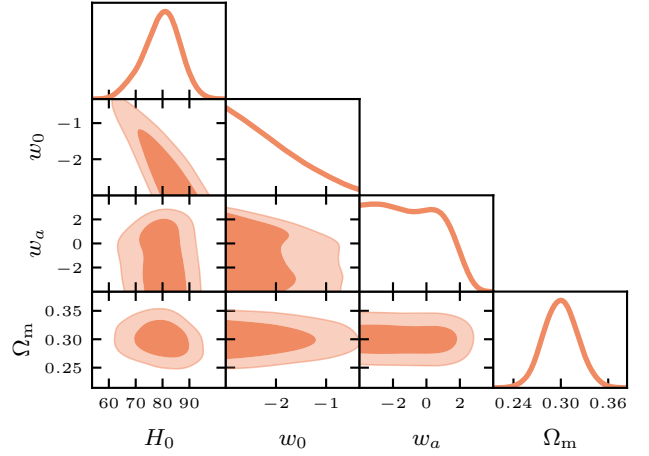


Figure 3. The one and two-dimensional marginalised posterior distributions of H_0 [$\text{kms}^{-1}\text{Mpc}^{-1}$], w_0 , w_a and Ω_m in a w_0w_a CDM cosmology from the seven TDCOSMO + 33 SLACS lenses.

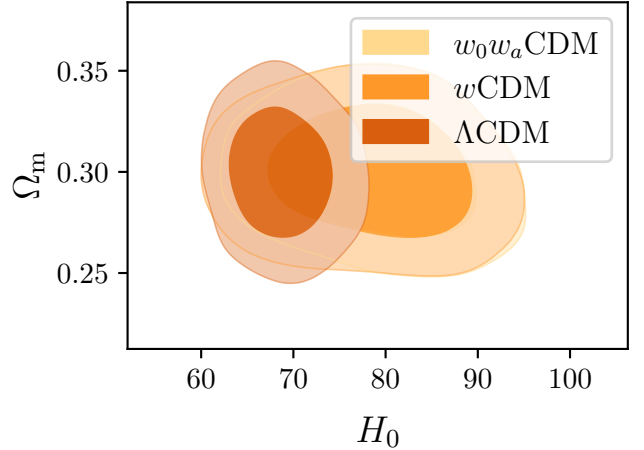


Figure 4. The two-dimensional marginalised posterior distributions of H_0 [$\text{kms}^{-1}\text{Mpc}^{-1}$] and Ω_m in the three cosmologies studied from the seven TDCOSMO + 33 SLACS lenses.

problematic depending on the specific cosmological model (Rubakov 2014).

4.3 w_0w_a CDM

In Figure 3, I show the one and two-dimensional marginalised posterior distributions of H_0 , w_0 , w_a and Ω_m in a w_0w_a CDM cosmology from the seven TDCOSMO + 33 SLACS lenses. The likelihood is again only able to provide loose upper limits on the dark energy equation of state parameters, $w_0 < -1.86$ and $w_a < 0.102$ at 68% confidence, and $w_0 < -0.861$, $w_a < 1.97$ at 95% confidence. Again the value of H_0 is larger than but still consistent with the Λ CDM measurement: $H_0 = 79.6^{+7.5}_{-6.0}$.

In Figure 4, I show the two-dimensional marginalised posterior distributions of H_0 and Ω_m in a Λ CDM cosmology (red), a w CDM cosmology (orange) and a w_0w_a CDM cosmology (yellow) from the seven TDCOSMO + 33 SLACS lenses. From this plot, it is clear that

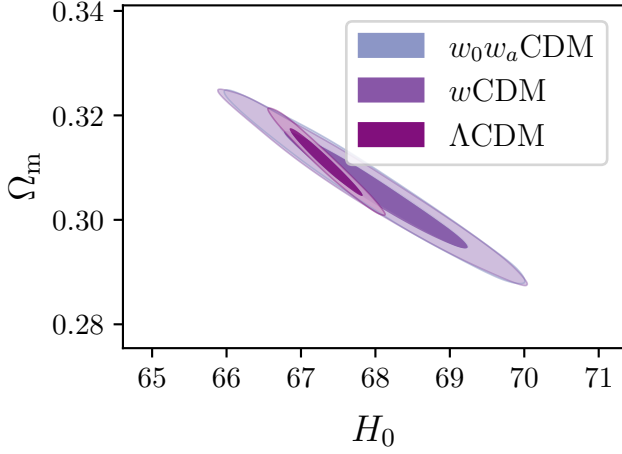


Figure 5. The two-dimensional marginalised posterior distributions of H_0 [$\text{kms}^{-1}\text{Mpc}^{-1}$] and Ω_m in the three cosmologies studied from the full combination of Planck 2018 + BAO + Pantheon SNIa + TDCOSMO + SLACS.

whilst the H_0 values in the extended cosmologies are large, they are still consistent at 1σ with the ΛCDM result.

It is important to note that my results are very similar to those found by Wong et al. (2020). This similarity implies that, for the six original H0LICOW lenses, the true lensing potential of each lens is well-approximated by the analytic profiles used in that work i.e. the mass-sheet degeneracy is making little contribution to the uncertainty on the cosmological parameters. Nevertheless, this may not be true for every lens in the Universe, and therefore the hierarchical likelihood procedure developed in Birrer et al. (2020) is the one which should be used for future cosmological inference involving strong lensing time delays.

4.4 Full combination of data

In Figure 5, I show the two-dimensional marginalised posterior distributions of H_0 and Ω_m in a ΛCDM cosmology (dark purple), a $w\text{CDM}$ cosmology (medium purple) and a $w_0 w_a \text{CDM}$ cosmology (light purple) from the full combination of Planck 2018 + BAO + Pantheon SNIa + TDCOSMO + SLACS data. In this case, I did not use the Pantheon prior on Ω_m , since the inclusion of the Pantheon dataset provides the same information as that prior. From this plot we can see that the values of H_0 and Ω_m in the extended cosmologies are completely consistent with the ΛCDM values at 1σ when using the full combination of data; the $w\text{CDM}$ and $w_0 w_a \text{CDM}$ constraints are virtually identical.

Furthermore, this combination of data inevitably provides a much stronger constraint on w , w_0 and w_a than the TDCOSMO + SLACS data alone, and removes any hint of a phantom dark energy component. In a $w\text{CDM}$ cosmology, the dark energy equation of state is measured to be $w = -1.025 \pm 0.029$, a marginal increase in precision compared to the Planck 2018 + BAO + SNIa value of $w = -1.028 \pm 0.031$. Both of these measurements are consistent with a cosmological constant.

In a $w_0 w_a \text{CDM}$ cosmology, $w_0 = -0.985^{+0.071}_{-0.091}$ and $w_a = -0.18^{+0.33}_{-0.25}$, compared to $w_0 = -0.957 \pm 0.08$ and $w_a = -0.29^{+0.32}_{-0.26}$ from Planck 2018 + BAO + SNIa. These are again both almost equivalent in precision and consistent with a cosmological constant. This

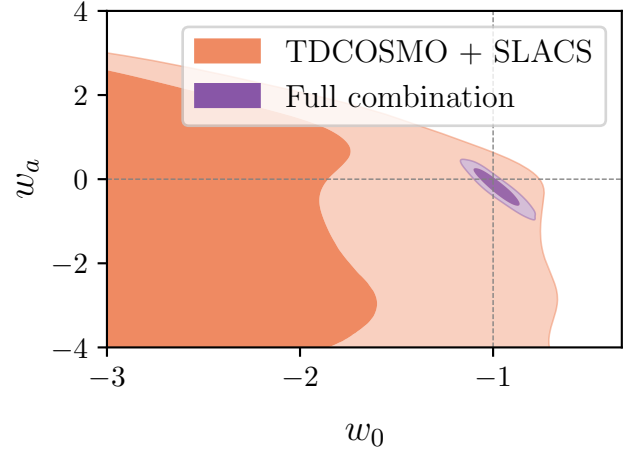


Figure 6. The two-dimensional marginalised posterior distributions of w_0 and w_a from the TDCOSMO + SLACS data (red) and from the full combination of Planck 2018 + BAO + Pantheon SNIa + TDCOSMO + SLACS (purple). The dashed lines show the values of these parameters which correspond to a cosmological constant, $w_0 = -1$, $w_a = 0$.

| Model | Data | χ^2 | d.o.f. | $\Delta\chi^2$ |
|----------------------|------------------|----------|--------|----------------|
| ΛCDM | TDCOSMO + SLACS | 114.2 | 9 | — |
| $w\text{CDM}$ | TDCOSMO + SLACS | 113.7 | 10 | -0.5 |
| $w_0 w_a \text{CDM}$ | TDCOSMO + SLACS | 113.5 | 11 | -0.7 |
| ΛCDM | Full combination | 4011.0 | 30 | — |
| $w\text{CDM}$ | Full combination | 4011.0 | 31 | 0.0 |
| $w_0 w_a \text{CDM}$ | Full combination | 4009.0 | 32 | -2.0 |

Table 2. The χ^2 , degrees of freedom, and $\Delta\chi^2$ values for each case studied.

can be clearly seen in Figure 6, where I show the two-dimensional marginalised posterior distributions of w_0 and w_a from the TDCOSMO + SLACS data (red) and from the full combination of Planck 2018 + BAO + Pantheon SNIa + TDCOSMO + SLACS (purple). The dashed lines in this plot show the values of the dark energy equation of state parameters which correspond to a cosmological constant, $w_0 = -1$ and $w_a = 0$.

Lastly, I computed the $\Delta\chi^2 \equiv \chi^2 - \chi^2_{\Lambda\text{CDM}}$ for each case studied. The computed values are shown in Table 2. Whilst the $\Delta\chi^2$ is negative for both extended cosmologies in the TDCOSMO + SLACS cases, implying that they are favoured over ΛCDM , the significance of this decrease in χ^2 must be evaluated using a difference table due to the greater number of degrees of freedom in the $w\text{CDM}$ cosmology with respect to ΛCDM . With one additional degree of freedom, and for a 95% level of significance, a $|\Delta\chi^2| > 3.841$ is required for the improvement in fit to be considered significant. This is clearly not the case here. From these results it is also evident that ΛCDM is a better fit to the full combination of data than the extended cosmologies, since the $\Delta\chi^2$ is on parity with ΛCDM in the $w\text{CDM}$ case and still does not exceed 3.841 for the $w_0 w_a \text{CDM}$ case.

5 CONCLUSIONS

In this work, I presented the first constraints on the equation of state of dark energy from the seven TDCOSMO lenses plus 33 SLACS lenses using the hierarchical likelihood provided by TDCOSMO. I wrote an external likelihood package for the Cobaya software, making this likelihood readily available for public use in combination with other cosmological likelihoods and theory codes.

I replicated the original TDCOSMO results in a Λ CDM cosmology and then explored two extended cosmologies, finding that the TDCOSMO + SLACS data was not able to place strong constraints on the equation of state of dark energy, obtaining only weak upper limits on w , w_0 and w_a . The constraints I obtained all implied the presence of a phantom dark energy component, $w < -1$, at 68% confidence.

The use of the TDCOSMO likelihood in combination with the Planck 2018 likelihood, BAO data and the Pantheon SNIa catalogue yielded more precise constraints, with all the dark energy equation of state parameters consistent with a cosmological constant, $w = -1$. I computed the $\Delta\chi^2$ to evaluate the fit of each model, finding no preference for the extended cosmologies over the Λ CDM case.

In conclusion, while strong lensing time delays are beginning to provide a competitive (albeit lens-modelling-dependent) measurement of H_0 , it is clear from the results of this work, which, in line with expectations from previous literature, indicate that other probes are more useful when studying dark energy. To improve the strong lensing time delay constraint, a larger dataset is certainly needed; perhaps on the order of hundreds or thousands of lenses (Shiralilou et al. 2020). Furthermore, an increase in precision on the H_0 inference will naturally lead to a reduction in the effect of the geometrical degeneracy which is contributing to the hints of phantom dark energy in the TDCOSMO data. Fortunately a number of current or near-future experiments, such as JWST, Roman, LSST and Euclid are likely to provide such data in abundance (Collett 2015).

ACKNOWLEDGEMENTS

I am grateful to Simon Birrer, Martin Millon and Judit Prat for valuable discussions about the TDCOSMO likelihood, and to Pierre Fleury for his comments on the manuscript.

DATA AVAILABILITY

All data associated with this article is publicly available.

REFERENCES

Aghanim N., et al., 2020a, *Astronomy & Astrophysics*, 641, A5
 Aghanim N., et al., 2020b, *Astronomy & Astrophysics*, 641, A6
 Aghanim N., et al., 2020c, *Astronomy & Astrophysics*, 641, A8
 Alam S., et al., 2017, *Monthly Notices of the Royal Astronomical Society*, 470, 2617
 Amendola L., et al., 2018, *Living Reviews in Relativity*, 21, 2
 Beutler F., et al., 2011, *Monthly Notices of the Royal Astronomical Society*, 416, 3017
 Birrer S., et al., 2020, *Astronomy & Astrophysics*, 643, A165
 Buen-Abad M. A., Fan J., Sun C., 2022, *Journal of High Energy Physics*, 02, 103
 Chan J. H. H., Rojas K., Millon M., Courbin F., Bonvin V., Jauffret G., 2021, *Astronomy & Astrophysics*, 647, A115

Chevallier M., Polarski D., 2001, *International Journal of Modern Physics D*, 10, 213
 Colaço L. R., Gonzalez J. E., Holanda R. F. L., 2021, *The European Physical Journal C*, 81, 533
 Colgáin E. O., Sheikh-Jabbari M. M., 2021, *Classical and Quantum Gravity*, 38, 177001
 Collett T. E., 2015, *The Astrophysical Journal*, 811, 20
 Copeland E. J., Sami M., Tsujikawa S., 2006, *International Journal of Modern Physics D*, 15, 1753
 Efstathiou G., Bond J. R., 1999, *Monthly Notices of the Royal Astronomical Society*, 304, 75
 Escamilla L. A., Giarè W., Di Valentino E., Nunes R. C., Vagnozzi S., 2023 (arXiv:2307.14802)
 Falco E. E., Gorenstein M. V., Shapiro I. I., 1985, *The Astrophysical Journal Letters*, 289, L1
 Fang W., Hu W., Lewis A., 2008, *Physical Review D*, 78, 087303
 Howlett C., Lewis A., Hall A., Challinor A., 2012, *Journal of Cosmology and Astroparticle Physics*, 1204, 027
 Lewis A., 2013, *Physical Review D*, 87, 103529
 Lewis A., 2019 (arXiv:1910.13970)
 Lewis A., Bridle S., 2002, *Physical Review D*, 66, 103511
 Lewis G. F., Ibata R. A., 2002, *Monthly Notices of the Royal Astronomical Society*, 337, 26
 Lewis A., Challinor A., Lasenby A., 2000, *The Astrophysical Journal*, 538, 473
 Linder E. V., 2003, *Physical Review Letters*, 90, 091301
 Motta V., García-Aspeitia M. A., Hernández-Almada A., Magaña J., Verdugo T., 2021, *Universe*, 7, 163
 Neal R. M., 2005 (arXiv:math/0502099)
 Perlmutter S., et al., 1999, *The Astrophysical Journal*, 517, 565
 Refsdal S., 1964, *Monthly Notices of the Royal Astronomical Society*, 128, 307
 Riess A. G., et al., 1998, *The Astronomical Journal*, 116, 1009
 Ross A. J., Samushia L., Howlett C., Percival W. J., Burden A., Manera M., 2015, *Monthly Notices of the Royal Astronomical Society*, 449, 835
 Rubakov V. A., 2014, *Physics-Uspekhi*, 57, 128
 Schneider P., Sluse D., 2013, *Astronomy & Astrophysics*, 559, A37
 Schneider P., Sluse D., 2014, *Astronomy & Astrophysics*, 564, A103
 Scolnic D. M., et al., 2018, *The Astrophysical Journal*, 859, 101
 Shiralilou B., Martinelli M., Papadomanolakis G., Peirone S., Renzi F., Silvestri A., 2020, *Journal of Cosmology and Astroparticle Physics*, 04, 057
 Sonnenfeld A., 2018, *Monthly Notices of the Royal Astronomical Society*, 474, 4648
 Torrado J., Lewis A., 2021, *Journal of Cosmology and Astroparticle Physics*, 05, 057
 Walsh D., Carswell R. F., Weymann R. J., 1979, *Nature*, 279, 381
 Wang L.-F., Zhang J.-H., He D.-Z., Zhang J.-F., Zhang X., 2022, *Monthly Notices of the Royal Astronomical Society*, 514, 1433
 Wong K. C., et al., 2020, *Monthly Notices of the Royal Astronomical Society*, 498

This paper has been typeset from a $\text{\TeX}/\text{\LaTeX}$ file prepared by the author.